



Original Full Length Article

Novel anatomic adaptation of cortical bone to meet increased mineral demands of reproduction



Carolyn M. Macica^a, Helen E. King^{b,c}, Meina Wang^d, Courtney L. McEachon^d, Catherine W. Skinner^b, Steven M. Tommasini^{d,*}

^a Department of Medical Sciences, Frank H. Netter, M.D., School of Medicine at Quinnipiac University, North Haven, CT 06518, United States

^b Department of Geology and Geophysics, Yale University, New Haven, CT 06520, United States

^c Department of Earth Sciences, Utrecht University, Utrecht, The Netherlands

^d Department of Orthopaedics and Rehabilitation, Yale University, New Haven, CT 06520, United States

ARTICLE INFO

Article history:

Received 9 July 2015

Revised 14 December 2015

Accepted 18 December 2015

Available online 26 January 2016

Keywords:

XLH

Pregnancy

Lactation

Carbonate

Phosphate

Cortical bone remodeling

Vitamin D

Osteoporosis

Mineral metabolism

MMP-13

ABSTRACT

The goal of this study was to investigate the effects of reproductive adaptations to mineral homeostasis on the skeleton in a mouse model of compromised mineral homeostasis compared to adaptations in control, unaffected mice. During pregnancy, maternal adaptations to high mineral demand include more than doubling intestinal calcium absorption by increasing calcitriol production. However, calcitriol biosynthesis is impaired in HYP mice, a murine model of X-linked hypophosphatemia (XLH). In addition, there is a paucity of mineralized trabecular bone, a primary target of bone resorption during pregnancy and lactation. Because the highest density of mineral is in mature cortical bone, we hypothesized that mineral demand is met by utilizing intracortical mineral reserves. Indeed, analysis of HYP mice revealed dramatic increases in intracortical porosity characterized by elevated serum PTH and type-I collagen matrix-degrading enzyme MMP-13. We discovered an increase in carbonate ion substitution in the bone mineral matrix during pregnancy and lactation of HYP mice, suggesting an alternative mechanism of bone remodeling that maintains maternal bone mass during periods of high mineral demand. This phenomenon is not restricted to XLH, as increased carbonate in the mineral matrix also occurred in wild-type mice during lactation. Taken together, these data suggest that increased intracortical periacicular mineral turnover also contributes to maintaining phosphate levels during periods of high mineral demand. Understanding the mechanisms of skeletal contribution to mineral homeostasis is important to improving the treatment and prevention of fracture risk and bone fragility for female patients with XLH, but also provides important insight into the role and unique adaptations of the maternal skeleton to the demands of fetal development and the needs of postnatal nutrition.

© 2016 Elsevier Inc. All rights reserved.

1. Introduction

Pregnancy and lactation require mobilization of mineral to provide to the offspring and several physiologic and metabolic adaptations occur to supply the required mineral [1,2]. Bone resorption provides much of the mineral during lactation. However, the effects on maternal bone metabolism during pregnancy have been largely unexplored and may involve short-term fragility and depletion of skeletal mineral content. During pregnancy, maternal adaptations to high mineral demand include more than doubling intestinal calcium absorption [2]. This process is mediated by 1,25(OH)₂D and possibly other factors [1]. Total

1,25(OH)₂D levels more than double during the first trimester and levels remain elevated until term [3]. However, free 1,25(OH)₂D levels do not increase until the third trimester when 80% of the calcium gained by the fetal skeleton is actively transferred across the placenta [2–4]. PTH falls to the lower end of the normal range [5–8], potentially protecting the maternal skeleton from excessive bone resorption [9]. Therefore, PTH is not the source driving the increase in 1,25(OH)₂D. Instead, other regulators of 1 α -hydroxylase must account for most of the circulating 1,25(OH)₂D during pregnancy [10].

In women with low dietary intake of calcium and vitamin D, PTH concentrations do not drop during pregnancy [11]. Thus, in certain cases, the maternal skeleton may contribute substantial amounts of calcium to the fetus. While the reliance on mineral from the maternal skeleton during pregnancy normally does not cause long-term changes in skeletal calcium content or strength [12], the effects of high mineral demand during pregnancy on maternal bone metabolism in patients with an already compromised mineral metabolism are not fully understood. Specifically, studies on the effects of pregnancy on mineral and bone

* Corresponding author at: Department of Orthopaedics and Rehabilitation, Yale University, 330 Cedar Street, FMB 554, P.O. Box 208071, New Haven, CT 06520-8071, United States.

E-mail addresses: carolyn.macica@quinnipiac.edu (C.M. Macica), H.E.King@uu.nl (H.E. King), meina.wang@yale.edu (M. Wang), courtney.mceachon@yale.edu (C.L. McEachon), catherine.skinner@yale.edu (C.W. Skinner), steven.tommasini@yale.edu (S.M. Tommasini).

metabolism in patients with X-linked hypophosphatemia (XLH) have not been conducted. XLH, an X-linked dominant disorder, is the most common form of familial hypophosphatemia, affecting an estimated 1 in 20,000 [13]. Patients with XLH suffer from aberrant regulation of 1,25(OH)₂D production leading to impaired intestinal calcium and phosphorus absorption and skeletal abnormalities characterized by defective calcification of cartilage and bone [14–16]. In addition, despite therapy with phosphate salts and active vitamin D, osteomalacia is not resolved and persists throughout adulthood [17]. Further, fibroblastic growth factor-23 (FGF-23), which is predominantly expressed in bone, stimulates renal phosphate wasting and impairs production of 1,25(OH)₂D in vivo [18].

In the current study, we investigated these reproductive adaptations to mineral homeostasis in a mouse model of XLH and control, unaffected mice. The HYP mouse of the C57BL/6 strain is a murine model that genocopies and phenocopies human XLH, making HYP mice ideal for studying the effects of impaired mineral homeostasis [17,18]. Mating of HYP females to C57BL/6 males produces both HYP and skeletally normal wild-type pups. Enormous mineral demand during pregnancy combined with the impaired intestinal phosphorous and calcium absorption in HYP mice could potentially increase the risk of fracture and contribute to the long-term compromise of the adult skeleton [14] as the skeleton would appear to be a reservoir by which pregnant and lactating patients with XLH maintain mineral metabolism. Further, because a murine model of XLH has decreased number of osteoclasts [19] and osteoclast activity [20], alternative forms of bone remodeling may be required to mobilize mineral [21]. Thus, the HYP mouse model offers two benefits in studying the skeletal contributions to mineral homeostasis: 1) improving our understanding on the impact of pregnancy and lactation on bone quality in patients with XLH for whom there are no definitive protocols for management and 2) studying alternative mechanisms for bone remodeling using the unusual combination of high mineral demand and impaired mineral homeostasis. By studying mineral and bone metabolism in both HYP and control mice, we aim to better our understanding of the interactions of vitamin D, mineral homeostasis and PTH on bone strength, providing an evidence-based rationale for improved clinical management of XLH during the reproductive years.

2. Materials and methods

Mice were fed standard chow ad libitum and tap water. All mice were maintained in accordance with the recommendations in the Guide for the Care and Use of Laboratory Animals and procedural protocol was approved by Yale's Institutional Animal Care and Use Committee. The study was split into 2 parts – pregnancy and lactation.

2.1.1. Generation of pregnant mice

HYP mice were obtained from colonies maintained by our laboratory. At 12 weeks of age, female C57BL/6J wild-type (WT) and HYP mice ($n = 8/\text{group}$) were bred to WT males. With HYP mice, litters are smaller in number. However, mating of HYP females to WT males produces both HYP and skeletally normal wild-type pups. Pregnant females were identified by the first appearance of a vaginal plug (designated as embryonic day 0.5 [E0.5]). Dynamic changes in femoral bone mineral density (BMD, g/cm^2) were measured by dual-energy X-ray absorptiometry using a PIXImus densitometer (Lunar, Madison, WI) 2 days before mating (baseline) and on E3, E10, E16, and after giving birth (E18.5). Immediately after giving birth, mice were killed, the femora and tibiae were harvested, cleaned of soft tissue, and analyzed as described below.

2.1.2. Generation of lactating mice

At 12 weeks of age, female WT and HYP mice were separated into the following groups ($n = 4\text{--}6/\text{group}$): 1) Lactating HYP, 2) Virgin HYP, 3) Lactating WT, 4) Virgin WT. Mice in the lactating groups were

paired with WT males for breeding. At the end of a 21-day lactation period post-partum, mice were killed, the femora and tibiae were harvested, cleaned of soft tissue and analyzed as described below.

2.2. High-resolution micro-computed tomography (HR micro-CT)

The mid-diaphysis of the right femur was scanned via phoenix nanotom® nano-CT (GE Measurement & Control Solutions, Longmont, CO, USA) at 1.55 μm resolution. At the selected resolution, both large pores such as vascular canals and small pores such as osteocyte lacunae are readily visible. To avoid potential bias associated with differences in the degree of mineralization between groups, images were individually thresholded to segment bone tissue from porosity and soft tissue via a standard thresholding algorithm [22], rather than using a global threshold. The resulting binarized images were then inverted for the quantification of porosities. To decrease errors associated with the limits of spatial resolution, pores with a volume less than 5 μm^3 were excluded. Cannular structures representing vasculature and/or bone remodeling units within cortical bone were classified as objects greater than 1000 μm^3 in volume [23]. Parameters measured included cannular volume (Ca.V) and cannular volume density (cannular volume per total cortical bone volume; Ca.V/TV). Porosity comprising the osteocyte lacunar system was classified as objects 100–1000 μm^3 in volume. Osteocyte lacunar indices included number of lacunae (Lc.N), lacuna number density (number of lacunae per total cortical bone volume; Lc.N/TV), total lacuna volume (Lc.V), lacuna volume density (Lc.V/TV), and average lacuna volume ($\langle \text{Lc.V} \rangle = \text{Lc.V}/\text{Lc.N}$). Percent porosity was defined as the total pore volume per total cortical bone volume.

2.3. Histology and immunohistochemistry

To explore potential mechanisms for bone remodeling, histological assessment of the bone was done to describe changes in cellular activity. Histological preparation was conducted at the Yale Orthopaedics Histology Lab. At death, right tibiae were rapidly dissected and fixed in 4% buffered paraformaldehyde for immunohistochemistry (IHC) staining for tartrate-resistant acid phosphatase (TRAP). IHC staining for alkaline phosphatase (ALP) activity was also used to detect and confirm the presence of intracortical vascular channels as described previously [24]. MMP-13 is a collagen matrix-degrading enzyme shown to be important in bone remodeling and in lactation-induced osteocytic remodeling [25]. We therefore assessed evidence of mineral mobilization by osteocytes by IHC staining of matrix metalloproteinase-13 (MMP-13) with a mouse anti-rat MMP-13 monoclonal antibody, as previously described [14]. After HR micro-CT, the right femora were embedded in poly(methyl methacrylate) (PMMA) and stained using von Kossa stain as previously described [14]. Measurement of areas of unmineralized matrix (osteoid volume/total volume; OV/TV) was performed on von Kossa stained slides of diaphyseal cortical bone and analyzed using Osteomeasure software (Osteometrics, Atlanta, GA).

2.4. Serum biochemical measurements

Blood was collected from the retro-orbital sinus of all pregnant mice at baseline, E3, E10, E16, and after giving birth (E18.5). Serum phosphorus was measured using a commercially available Liqui-UV kit (Stanbio, Boerne, TX). Serum phosphorous was not measured at in WT mice at E16 because of inadequate amounts to perform all assays. Serum calcium was assessed using Sigma kits employing a plate reader (Titertek Multiscan, Huntsville, AL). 1,25(OH)₂D was measured using a commercially available RIA kit (DiaSorin, Stillwater MN). Parathyroid hormone (PTH) was measured using a two site ELISA that employs antimouse PTH antibodies and intact rat PTH standards (Alpco, Salem, NH) [26].

2.5. Matrix chemical composition determined by Raman spectroscopy

Mineral substitutions into the hydroxyapatite lattice are important to crystal size, density, and solubility and abnormal bone mechanical properties have been correlated with abnormal carbonate content, an anionic substituent of phosphate, in bone [27–29]. Left femoral diaphyses were analyzed using Raman spectroscopy to measure average chemical composition within the cortical bone. Raman spectra were collected from longitudinal cross-sections of bones embedded in PMMA. We used a Horiba HR500 micro-Raman spectrometer equipped with an Olympus BX-41 light microscope. The 532 nm laser was used for Raman analysis along with a 100× objective lens and 300 μm confocal

hole providing a spot size of ~1 μm at the sample surface. The backscattered light passed through a 100 μm slit before being dispersed by an 1800 grooves/mm grating and collected by a charge coupled device. Four regions of interest located within the diaphysis were examined for each bone. As bone is a very inhomogeneous material, 16 individual spectra were collected in each area and the results compiled to obtain a representative average of the bone composition. To prevent the cortical bone from burning due to the interaction of the laser beam with the bone tissue, a 0.6 optical density filter was used to lower the intensity of the laser beam at the sample surface. Each spectrum was collected for 30 s and integrated 10 times to obtain adequate signal to noise ratios. The surface of the sample was imaged using the optical

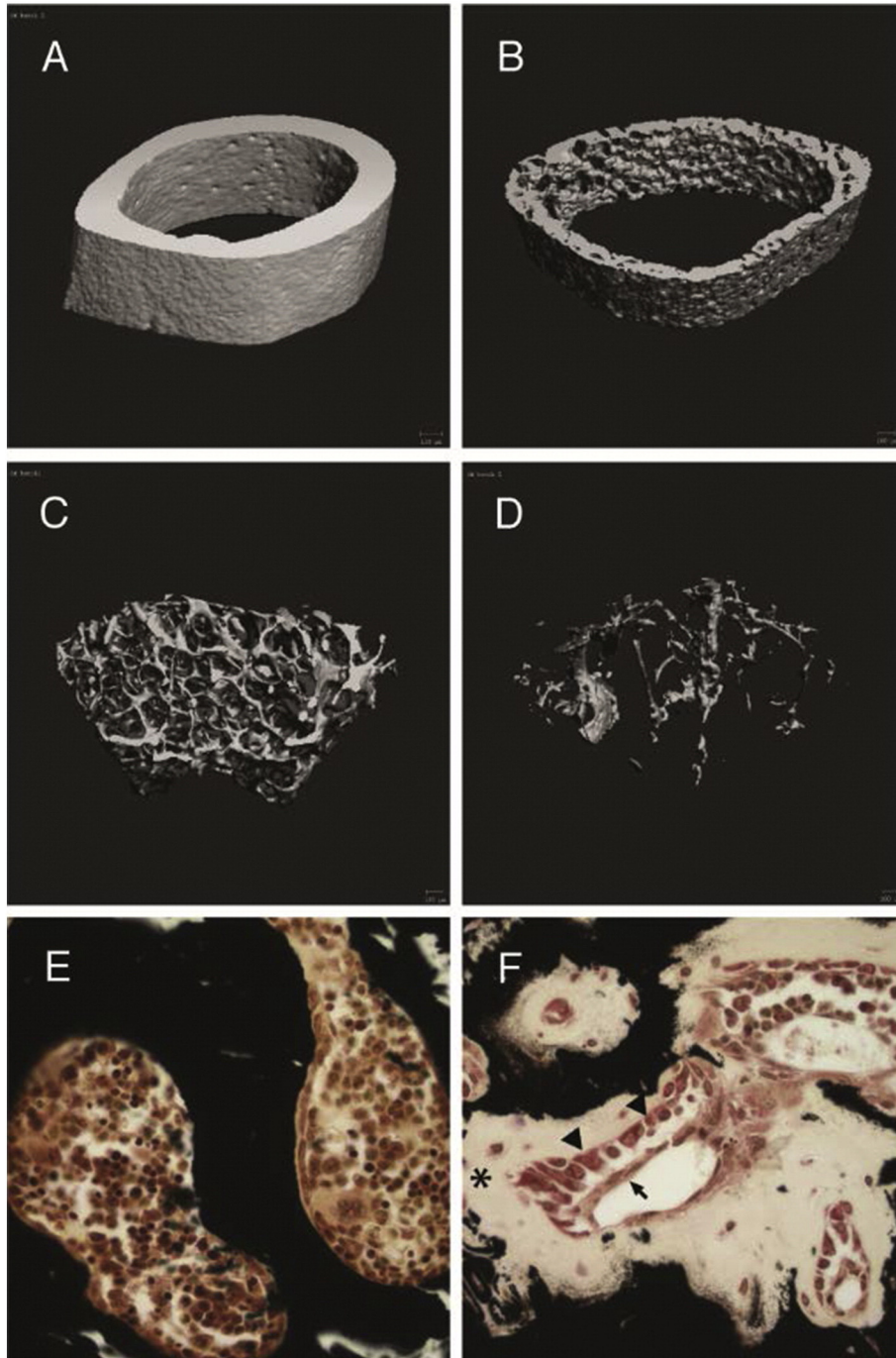


Fig. 1. (A–D) Micro-CT of proximal tibia cortical and trabecular bone for virgin WT (A–B) and HYP (C–D) mice show increased apparent cortical porosity and paucity of trabecular bone in HYP mice. (E–F) Von Kossa staining shows metabolically active osteoblasts (arrow head) covered by canopy cells (arrow) involved in the synthesis and secretion of matrix. Failure of this matrix to mineralize in HYP mice (F) demonstrates osteomalacia (black*) relative to WT (E).

microscope on the Raman before and after the measurement to ensure that the sample had not reacted with the laser during acquisition. To minimize the laser exposure of the bone tissue, each spectrum was acquired only in the spectral region of interest of 800–1200 cm^{-1} . The contribution of the carbonate symmetrical stretching peak at 1074 cm^{-1} was determined using the method described in Awonusi et al. 2008 [30].

2.6. Spatial distribution of matrix composition and MMP-13 expression

The spatial distribution of carbonate substitution, collagen-cross linking, and MMP-13 expression was quantified as a function of distance from osteocyte lacunae. First, in order to map the matrix composition changes, a field of view larger than that possible with Raman spectroscopy was needed. This was achieved by using synchrotron-based Fourier transform infrared microspectroscopy. Left femoral diaphyses were embedded in PMMA and longitudinal sections (4 μm thin) were analyzed with FTIR-I at Brookhaven National Laboratory National Synchrotron Light Source (NSLS) U10B beam line. A spectrophotometer, with a Hyperion IR microscope (Bruker, Billerica, MA) with an MCT detector was used in a frequency range of 4000 to 650 cm^{-1} via spectral mapping. Spectra were collected at 128 scans per point in transmission mode. Four 64 μm \times 64 μm regions of interest (ROI) were analyzed. Data were collected and processed using Opus software (Bruker, Billerica, MA). Absorbance data were analyzed for average mineralization (phosphate/protein ratio), collagen cross-linking, and carbonate substitution. Next, the carbonate substitution and collagen cross-linking as a function of distance from a pore's edge were determined. ROIs were isolated around pores in the synchrotron radiation-based FTIR maps and images of MMP-13 immunostaining. Using a custom Matlab (R2014b, MathWorks Inc., Natick, MA) algorithm, an isolated pore region (50 \times 50 μm) was extracted from each map/image and the pore edges were identified. Then for each point within the mineralized tissue, the shortest distance to the pore edge was calculated using a 2D Euclidian distance transform. Similarly, IHC-stained bone sections were used to quantify and map the stain intensity distribution of MMP-13 around pores. Rather than measure the intensity of each pixel, the IHC images were broken into smaller sub-matrices within which the average staining intensity of each sub-matrix was taken. Thus, using the staining intensity as a measure of MMP-13 expression, MMP-13 concentration was characterized as a function of the distance from the unmineralized pore.

2.7. Statistical analyses

All statistical analyses used GraphPad Prism software (GraphPad, San Diego, CA). To account for small sample size, statistical difference between lactating groups was determined using non-parametric ANOVA (Kruskal–Wallis) and Dunns post-hoc test. After confirming normal distribution of the data for pregnant mice, statistical differences between groups and time-points during pregnancy were determined using One-way ANOVA and Tukey post-hoc test. Significance was indicated at $p < 0.05$. All data are presented as mean \pm standard deviation.

3. Results

3.1. Changes in BMD and micro-porosity during pregnancy and lactation

Micro-CT analysis of HYP mice tibia confirmed an increase in cortical bone porosity and significantly diminished trabecular bone volume relative to virgin WT mice, both prototypical features of a phosphate wasting disorder (Fig. 1A–D). Maternal demands of mineral are largely dependent upon the trabecular network of bone. However, in HYP mice, there is a paucity of mineralized trabecular bone due to osteomalacia, with a failure of the extracellular matrix to mineralize in the hypophosphatemic environment (Fig. 1E vs. 1F). Because the highest density of mineral exists in cortical bone, we sought to examine the potential role of cortical bone as a mineral reserve to support pregnancy and lactation in HYP mice. Small animal dual-energy X-ray absorptiometry (DXA) proved to not have a sensitive enough resolution to measure the expected subtle longitudinal changes in cortical bone mass and porosity that occur during the short murine gestation. However, HR-micro-CT and von Kossa staining not only revealed significant differences between HYP and WT porosity, but significant changes during pregnancy and lactation (Table 1). Lactating WT showed increased porosity, compared to virgin and pregnant WT. However, although both WT and HYP mice showed slightly larger total osteocyte lacuna volume at the end of lactation compared to virgin controls, changes in osteocyte lacunar size $\langle \text{Lc.V} \rangle$ were too subtle for statistical significance (Table 1).

At both the end of pregnancy and after a 21-day lactation period, HYP overall porosity (% porosity) was increased by nearly 75% relative to virgin HYP ($p < 0.05$; Table 1). This increase in apparent porosity, measured as canal volume per total cortical bone volume (Ca.V/TV), was due to an increase in the proportion of large vascular and mineral-deficient cannular structures within the cortical bone. Pregnant and lactating HYP had increased Ca.V/TV relative to virgin HYP ($p < 0.05$; Table 1). It is important to note that we refer to this as “apparent” porosity because micro-CT does not distinguish between actual pores and regions of mineral-deficient bone matrix in cortical bone or surrounding osteocyte lacunae. The apparent porosity of cortical bone becomes evident by von Kossa staining, illustrating the corresponding pores of micro-CT as mineral-deficient matrix, or intracortical osteoid (OV/TV), and confirming the increase in porosity in HYP mice (Fig. 2A–D, Table 1).

3.2. Characterization of cortical bone porosity

Alkaline phosphatase (ALP) activity confirmed the presence of intracortical vascular channels in HYP mice [24]. ALP staining of cortical bone correlated with the cortical pores identified by HR-micro-CT (Fig. 2E). Phase contrast microscopy also revealed differences in the matrix immediately surrounding the intracortical canals of ALP-stained sections (Fig. 2F), consistent with the lack of mineral by von Kossa staining (Fig. 2C–D).

MMP-13 immunoreactivity in cortical bone was assessed to determine the contribution of matrix-degrading enzymes potentially involved in the liberation of bone matrix mineral and of vascular

Table 1
Intracortical microporosities as measured by high-resolution micro-CT and von Kossa staining.

| | % porosity | Ca.V/TV [%] | $\langle \text{Lc.V} \rangle$ [mm^3] | Lc.V/TV [%] | OV/TV [%] |
|---------------|------------------------------|------------------------------|---|-------------------------------|------------------------------|
| Virgin WT | 1.5 \pm 0.6* | 1.2 \pm 0.4* | 198.2 \pm 12.0* | 0.34 \pm 0.26 | N.D.* |
| Pregnant WT | 0.9 \pm 0.2* | 0.5 \pm 0.1* | 176.6 \pm 3.9* | 0.27 \pm 0.10 | N.D.* |
| Lactating WT | 3.4 \pm 0.4* ⁺ | 2.6 \pm 0.5* ⁺ | 219.3 \pm 15.0 | 0.73 \pm 0.02* ⁺ | N.D.* |
| Virgin HYP | 8.8 \pm 2.2* | 8.4 \pm 2.4* | 238.1 \pm 18.4* | 0.38 \pm 0.21 | 7.8 \pm 2.4* |
| Pregnant HYP | 14.5 \pm 1.2* ⁺ | 14.1 \pm 1.2* ⁺ | 233.7 \pm 4.6* | 0.30 \pm 0.02 | 21.9 \pm 6.1* ⁺ |
| Lactating HYP | 13.8 \pm 2.8* ⁺ | 13.5 \pm 2.8* ⁺ | 241.2 \pm 2.3 | 0.28 \pm 0.04* | 19.1 \pm 3.3* ⁺ |

N.D. – not detectable. n = 8/group: virgin, pregnant; n = 4–6/group: lactating. Data presented as mean \pm standard deviation.

* Significant difference between WT and HYP.

⁺ Significant difference from virgin ($p < 0.05$).

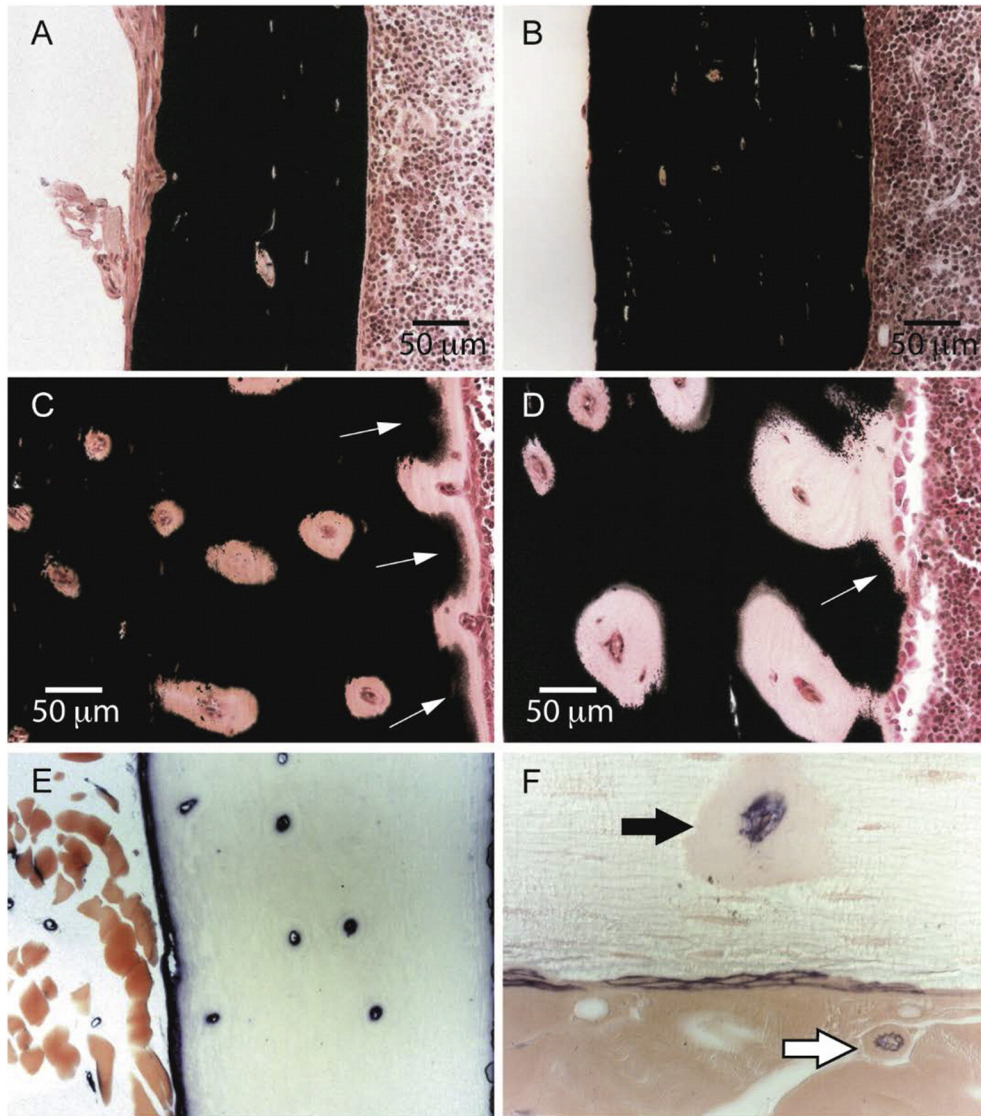


Fig. 2. (A–D) Von Kossa staining of cortical bone in virgin WT (A), lactating WT (B), virgin HYP (C), lactating HYP (D). The unmineralized matrix in cortical bone (unstained areas in C and D) in HYP is distinct from osteomalacia of the endosteal surface (arrows in C and D) which is populated with osteoblasts. (E) ALP staining for vasculature confirmed the increase in intracortical vascularization in HYP mice, also revealing vessels within muscle. (F) Phase contrast microscopy showing unmineralized bone matrix around ALP-staining (black arrow) and muscle vasculature (white arrow).

ingrowth. MMP-13 immunoreactivity was higher in virgin HYP compared to virgin WT ($p < 0.05$; Fig. 3A). At the end of pregnancy, MMP-13 expression was significantly increased in both WT and HYP mice relative to virgin mice ($p < 0.05$, Fig. 3A). MMP-13 remained elevated in HYP throughout lactation (Figs. 3A and 4A), but by the end of the 21-day lactation period had returned to baseline levels in WT mice (Fig. 3A).

To determine the potential contribution of TRAP-positive cells required to meet the mineral demands of pregnancy and lactation, we stained tibial sections for the presence of TRAP activity. Although TRAP staining is normally negligible in HYP mice, TRAP staining revealed that osteoclast activity in tibial cortical bone in HYP mice increased significantly during pregnancy ($p < 0.05$) and remained elevated during lactation (Figs. 3B and 4B–C).

3.3. Serum biochemistry during pregnancy

Despite a genetic disposition to elevated PTH and suppressed 1,25(OH)₂D, HYP mice had strikingly similar changes in maternal serum levels of PTH, 1,25(OH)₂D, calcium, and phosphorus as compared

to WT mice (Table 2; Fig. 5). Although a key feature of XLH is impaired 1,25(OH)₂D production, HYP mice showed significantly increased levels of circulating 1,25(OH)₂D during pregnancy (E16), similar to wild-type WT. At the end of pregnancy (E18.5), maternal serum levels of 1,25(OH)₂D had returned to baseline levels in both HYP and WT.

Another feature of XLH is elevated PTH. Indeed, PTH levels in HYP mice were more than double that of WT mice ($p < 0.05$). During pregnancy, PTH remained elevated in HYP compared to WT. However, by late pregnancy (E16), PTH levels in both HYP and WT mice dropped to 25% of the baseline levels. At the end of pregnancy (E18.5), PTH remained significantly lower than baseline levels in WT and HYP mice. However, PTH again began to increase during late pregnancy.

Maternal serum levels of calcium (Ca^{++}) were similar between WT and HYP mice over the course of pregnancy. Although not significantly different from baseline, both HYP and WT showed a further increase in serum Ca^{++} towards the end of pregnancy ($p > 0.05$) despite suppression of 1,25(OH)₂D, but consistent with elevation of PTH during this same time period. Maternal serum levels of phosphorus (P) were higher at baseline in WT compared to HYP mice. P levels in pregnant WT mice were relatively unchanged. However, maternal serum P levels

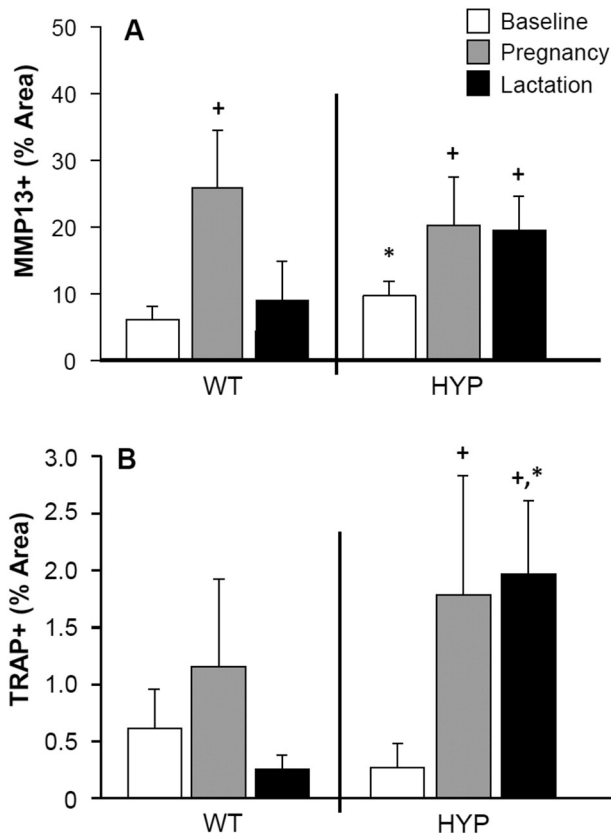


Fig. 3. (A) MMP-13 immunoreactivity was higher in HYP tibiae at baseline compared to WT tibiae. At the end of pregnancy, MMP-13 expression was increased in both WT and HYP. MMP-13 remained elevated in HYP throughout lactation, but by the end of the 21-day lactation period had returned to baseline levels in WT mice. (B) TRAP positive staining was increased in both WT and HYP tibiae during pregnancy and remained elevated only in HYP during lactation. ⁺ Significantly different from baseline controls; ^{*} Significant difference between WT and HYP. n = 8/group: virgin, pregnant; n = 4–6/group: lactating. All error bars indicate standard deviation.

were increased in HYP mice ($p < 0.05$) during late pregnancy (E16 and E18.5). This increase in serum P, indeed to near normal levels, was consistent with the increase in $1,25(\text{OH})_2\text{D}$ between baseline and E16. From E16 to E18.5, although still elevated, maternal serum P in HYP mice began to decrease consistent with the concomitant decrease in $1,25(\text{OH})_2\text{D}$.

3.4. Changes in cortical bone matrix composition as determined by Raman spectroscopy

Mineral substitutions into the hydroxyapatite lattice such as the anionic substitution of carbonate for phosphate impact crystal size, density, and solubility [30–32]. Because abnormal bone mechanical properties have been correlated with alterations in carbonate content in bone, we measured the carbonate to phosphate ratio in cortical bone given the hypophosphatemic environment. Analysis of cortical bone from HYP and WT mice by Raman spectroscopy revealed a significantly higher amount of carbonate ion substitution in HYP mice compared to WT (Fig. 6). Additionally, WT mice showed significant increases in carbonate ion substitution during lactation relative to baseline ($p < 0.001$). HYP mice also showed a similarly significant increase in carbonate ion substitution during lactation compared to pregnancy and baseline ($p < 0.001$). Taken together, these data suggest that the observed carbonate accumulation serves as a surrogate for calcium phosphate hydroxyapatite during periods of high mineral demand regardless of the presence or absence of familial phosphate-wasting.

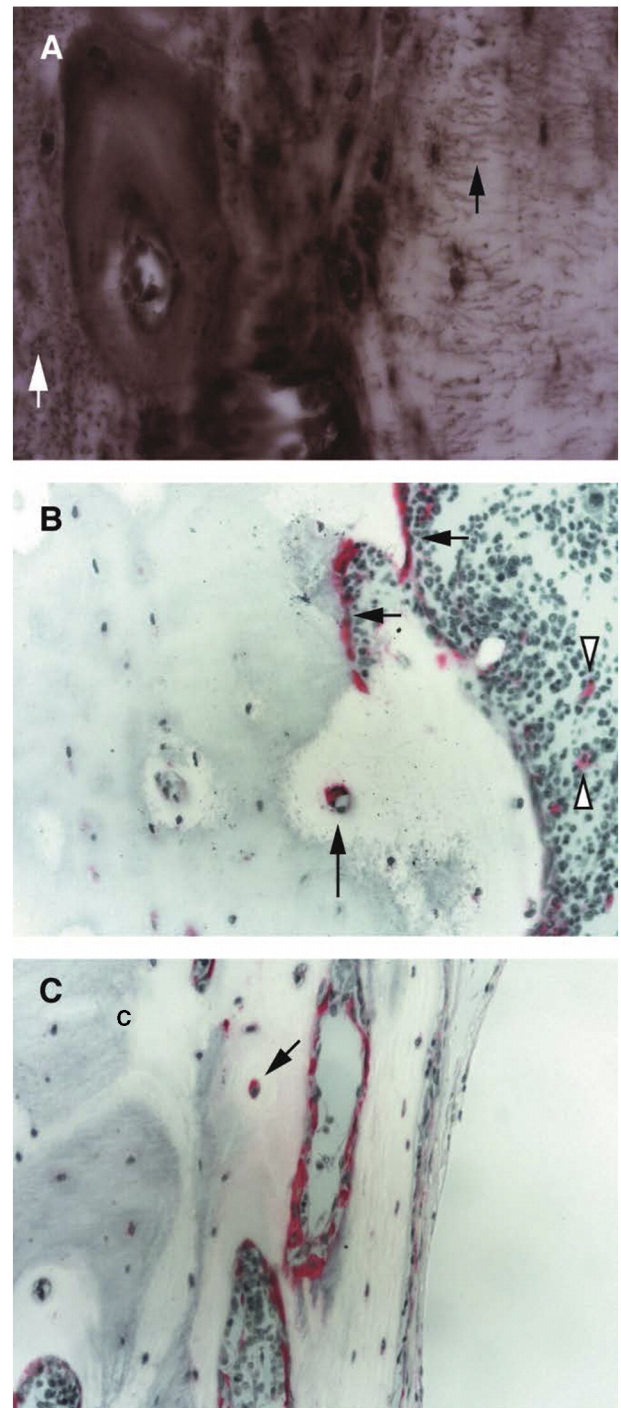


Fig. 4. (A) MMP-13 immunoreactivity in HYP mice tibiae showed intense MMP-13 (dark brown areas) coincident with areas of unmineralized matrix and with osteocyte canaliculi shown both longitudinally (black arrows) and in cross section (white arrows); (B) TRAP staining of HYP mice tibiae revealed increased intracortical TRAP activity with no associated osteoclast pit formation (arrow); TRAP activity is also shown along the endocortical surface and in bone marrow (stars); (C) frontal section captures TRAP activity along endocortical surfaces and with osteocyte soma. (For interpretation of the references to color in this figure legend, the reader is referred to the web version of this article.)

3.5. Spatial distribution of matrix composition and MMP-13 expression

To determine if osteocyte expression of MMP-13 was related to changes in the mineral matrix, we quantified the spatial distribution of carbonate substitution, collagen-cross linking, and MMP-13 expression

Table 2
Maternal serum biochemistry during pregnancy.

| | Baseline | E16 | E18.5 |
|---------------------------------|---------------|---------------------------|--------------------------|
| PTH [pg/mL] | | | |
| WT | 124.6 ± 34.3* | 48.3 ± 9.9 | 53.8 ± 15.2 |
| HYP | 267.8 ± 82.1* | 68.7 ± 23.6 ⁺ | 95.6 ± 47.7 ⁺ |
| 1,25(OH) ₂ D [pg/mL] | | | |
| WT | 202.4 ± 46.6 | 281.2 ± 48.4 | 129.8 ± 22.0 |
| HYP | 160.4 ± 31.0 | 259.4 ± 96.7 ⁺ | 134.5 ± 59.8 |
| Ca [mg/dL] | | | |
| WT | 7.9 ± 0.5 | 8.6 ± 1.0 | 9.0 ± 1.4 |
| HYP | 7.3 ± 0.6 | 8.1 ± 0.8 | 8.4 ± 0.6 |
| P [mg/dL] | | | |
| WT | 9.0 ± 1.0* | | 10.2 ± 0.5* |
| HYP | 6.6 ± 0.6* | 8.6 ± 0.5 ⁺ | 8.0 ± 1.0* ⁺ |

n = 8/group/time-point. Data presented as mean ± standard deviation.

* Significant difference between WT and HYP.

⁺ Significant difference from baseline ($p < 0.05$).

as a function of distance from osteocyte lacunae (Fig. 7). The highest levels of MMP-13 and carbonate substitution corresponded to alterations in collagen cross-linking and occurred within 5 to 10 μm of a pore. Quantitatively, carbonate substitution decayed exponentially as a function of distance, as did the ratio of reducible to non-reducible cross-links. Alterations in matrix composition occurred in both WT and HYP mice, but HYP mice had a 50% higher baseline of carbonate substitution in both the pregnant and lactating states. Together with the elevated expression of MMP-13 in HYP, the data point to a higher osteocyte-mediated contribution to mineral homeostasis in both WT and HYP mice.

4. Discussion

4.1. Maternal adaptations during pregnancy and lactation

The results of this study reveal that HYP mice deploy similar adaptations to mineral demand during pregnancy as wild-type mice. Consistent with a previous observation that 1,25(OH)₂D levels were not suppressed in HYP mice during pregnancy [33], we show that HYP mice upregulated 1,25(OH)₂D during pregnancy – this despite aberrant 1,25(OH)₂D biosynthesis due to tonic inhibition of 1 α -hydroxylase activity by FGF-23. Concomitant with an the increase in 1,25(OH)₂D, PTH decreased during pregnancy in HYP and WT mice. However, in HYP mice PTH remained elevated relative to WT and, at term (E18.5), PTH began to increase again, consistent with what is observed in human pregnancy. The late increase in PTH may be related to the onset of bone remodeling, which becomes the main source of mineral during lactation. The mechanism by which HYP mice upregulate 1,25(OH)₂D during pregnancy might include induction of a positive regulator of 1 α -hydroxylase or suppression of a negative regulator of 1 α -hydroxylase. It has been shown previously that FGF-23 remains significantly elevated during HYP pregnancy relative to WT [34]. Because FGF-23 levels remain elevated, it is unlikely that the suppression of FGF-23 contributes to the increase in 1,25(OH)₂D production.

Understanding the mechanism by which gestational 1,25(OH)₂D synthesis is significantly upregulated, and one that occurs in a disorder characterized by suppression of 1 α -hydroxylase activity, is important to improving our understanding of the complex maternal response to the metabolic demands of the developing fetus and breastfeeding infant. Because PTH is a positive regulator of the renal 1 α -hydroxylase gene (*Cyp27b1*) [2], upregulation of 1,25(OH)₂D levels in the face of diminishing levels of PTH is consistent with an alternative physiological stimulus for enhanced intestinal absorption during pregnancy. However, as we and others have shown, PTH is not responsible for the higher 1,25(OH)₂D levels during pregnancy [35]. Further, the factors involved in the upregulation of 1,25(OH)₂D in HYP mice are currently unknown. PTHrP may contribute to bone turnover during lactation [36] and has been proposed to play a role in the upregulation of 1,25(OH)₂D [35].

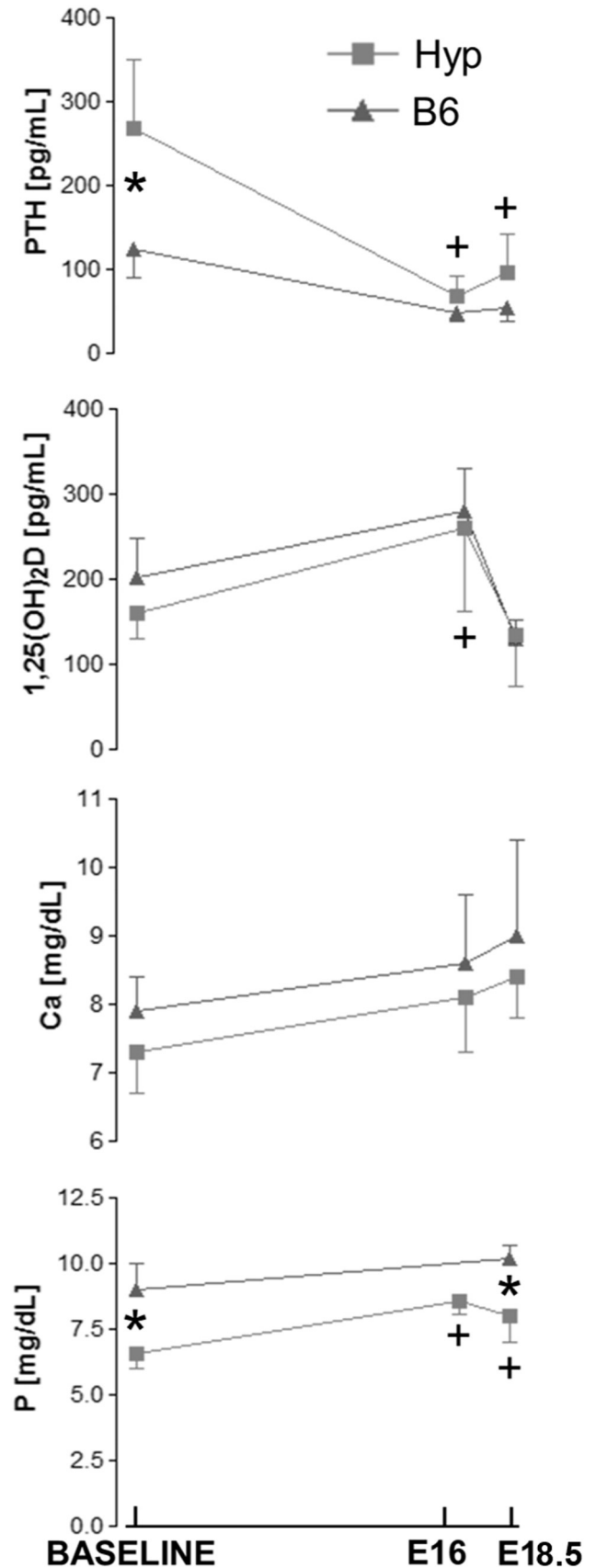


Fig. 5. Maternal serum biochemistry during pregnancy revealed similar adaptations to mineral demand between HYP and WT mice. ⁺ Significantly different from baseline controls; *Significant difference between WT and HYP ($p < 0.05$). n = 8/group; virgin, pregnant. All error bars indicate standard deviation.

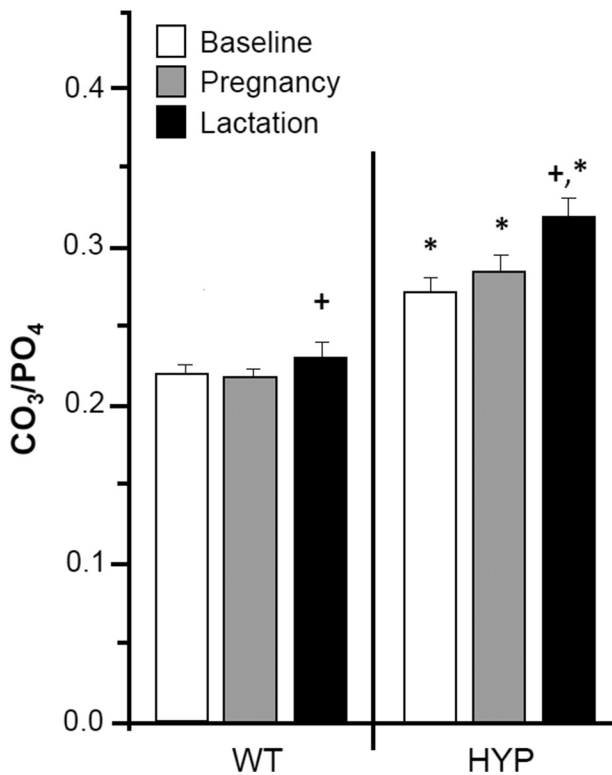


Fig. 6. Analysis of cortical bone from HYP and WT mice by Raman spectroscopy confirmed a significantly higher amount of carbonate ion substitution (CO_3/PO_4) in HYP mice compared to WT. Interestingly, WT mice showed significant increases in carbonate ion substitution during lactation relative to baseline controls ($p < 0.001$). + Significantly different from baseline controls; * Significant difference between WT and HYP. $n = 8$ /group: virgin, pregnant; $n = 4$ –6/group: lactating. All error bars indicate standard deviation.

However, it has been shown that the profile of PTHrP does not correlate with the induction of $1,25(\text{OH})_2\text{D}$ nor is it a potent activator of the renal *Cyp27b1* [37]. Other potential candidates include calcitonin and prolactin. Prolactin has been shown to potentiate the effects of vitamin D by directly stimulating intestinal calcium absorption and, additionally, stimulating expression of the renal *Cyp27b1* to facilitate vitamin D-dependent calcium and phosphate absorption [38–40]. Calcitonin, shown to be involved in protecting the maternal skeleton from excessive mineral loss during lactation, is a renal stimulator of 1α -hydroxylase and is unaffected by hypophosphatemia, thus highlighting its potential as a therapeutic for XLH [41–44].

During pregnancy, serum Ca^{++} and P levels rose, likely as a consequence of facilitated intestinal absorption mediated by the significant increase in $1,25(\text{OH})_2\text{D}$. During the latter stages of pregnancy (E16–E18.5), when there is a more significant accretion of mineral in the developing fetus, Ca^{++} levels continue to increase despite a significant reduction in $1,25(\text{OH})_2\text{D}$ levels. Together with our data showing a significant increase in cortical porosity in HYP mice, this suggests that the source of mineral is derived from cortical bone and independent of $1,25(\text{OH})_2\text{D}$. Thus, during this stage of pregnancy, there is a transition from vitamin D dependent absorption of mineral to the onset of skeletal resorption providing mineral for the full term fetus and continuing throughout lactation. This finding is not surprising given the paucity of mineralized bone in HYP mice (Fig. 1C–D) [26] as cortical bone represents the most significant source of bone mineral in the face of increased demand.

4.2. Skeletal adaptations during periods of high mineral demand

We propose an alternate mechanism of bone remodeling, which we refer to as “perilacunar mineral turnover” that preserves the maternal

skeleton during pregnancy. These data suggest that the bone mineral loss that typifies late pregnancy and lactation undergoes a de novo process in which phosphate (PO_4^{3-}) in the mineral matrix is replaced with carbonate (CO_3^{2-}) [31,32]. Incorporation of carbonate creates a more soluble apatite [45] which may underlie the remarkably rapid recovery of the skeletal integrity with calcium phosphate hydroxyapatite that occurs following cessation of lactation. Unlike other forms of bone loss where bone resorption exceeds formation such as weightlessness, glucocorticoid therapy and estrogen deficiency, this unique form of perilacunar mineral turnover seen during pregnancy is not associated with significant net mineral loss because of anionic substitution into the matrix. Our data suggest that this unique form of perilacunar mineral turnover is maintained during lactation even though PTH begins to increase and skeletal turnover with bone mineral loss commences. As there is little to no evidence of a significant increase in osteoporosis or fractures among women who have multiple pregnancies [46], and preliminary evidence in our lab shows no cumulative effect of carbonate incorporation after multiple pregnancies and lactations, this possible mechanism may be key to the rapid skeletal recovery with calcium phosphate and protection from osteoporosis after pregnancy and lactation.

These data may have important implications in maintaining phosphate levels in the clinical management of XLH in adulthood during periods of high mineral demand. The greatest loss of mineral during lactation occurs from the trabecular skeleton, especially from the trabecular-rich spine [47,48]. However, the mechanism for bone resorption in an already hypophosphatemic skeleton with low trabecular bone volume is unclear. Increased bone resorption on cortical surfaces may differ from bone resorption in trabecular bone during pregnancy and lactation in XLH. In HYP mice, osteoclast number is significantly decreased and the PHEX mutation and subsequent impaired mineralization process result in few mineralized surfaces for osteoclasts to resorb bone. Therefore, alternative mechanisms of bone resorption that either create new mineralized surfaces available for resorption by osteoclasts or free up matrix mineral independently of osteoclast activity are presumed to occur in pregnant XLH patients (and pregnant HYP mice).

Recent evidence has shown that osteocytes may directly contribute to mineral homeostasis [49,50]. It appears the osteocyte contribution works in conjunction with osteoclast-driven remodeling, becoming more prominent in cases where osteoclast resorption is impaired or demand is high [51–53]. Our data point to osteocyte expression of matrix metalloproteinase-13 (MMP-13), which degrades the collagen matrix, as a means of freeing mineral ions from the perilacunar matrix. This is consistent with other reports showing expression of MMP-13 to be required for osteocytic perilacunar remodeling [30]. MMP-13 null mice have altered primary ossification centers with delayed vascular penetration, suggested to be a result of VEGF sequestered in the cartilage matrix not being “released” in order to initiate vascularization [54,55]. Virgin HYP mice have elevated MMP-13 levels compared to virgin WT, and thus, we expect these elevated MMP-13 levels persist in pregnant HYP mice in order to degrade the collagenous matrix and allow for vascularization to occur. The ratio of reducible to non-reducible crosslinks was measured by the absorbance data from FTIR. Although the significance of the ratio of collagen cross-links is not fully understood, Paschalis et al. demonstrated that the ratio of crosslinks increased with distance from the forming trabecular surface, identified by visible osteoid, while remaining constant at resorbing surfaces of the bone in which osteoclast-mediated pits were evident [56]. Our data suggest that increased non-reducible cross-linking occurs co-locally with phosphate release from the bone and osteocyte-mediated MMP-13 expression. Thus, the changes in collagen cross-linking during lactation-induced mineral mobilization observed in this study are indicative of osteocyte- and not osteoclast-mediated adaptation to high mineral demand. However, the implications of collagen cross-linking changes during pregnancy and action require further study.

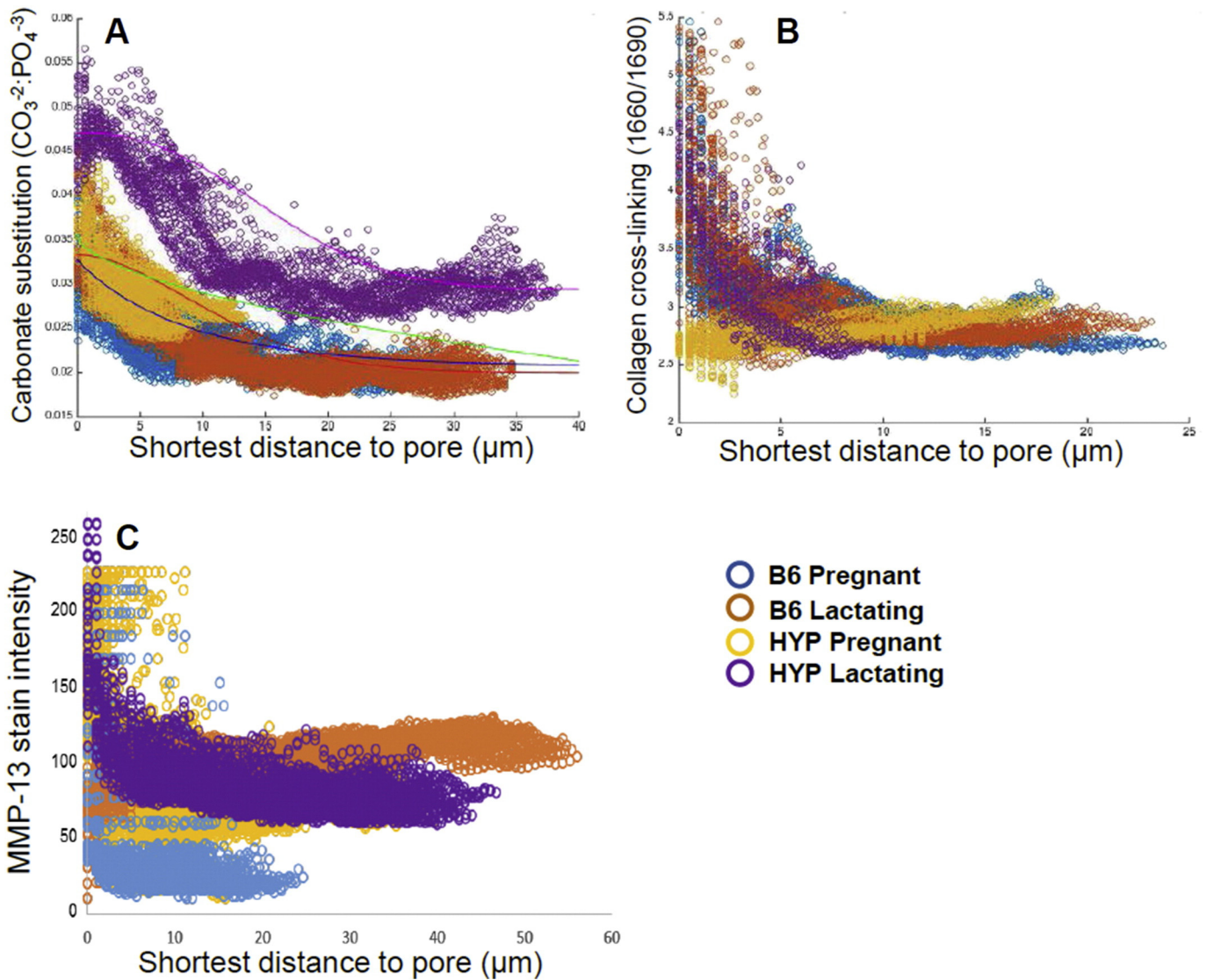


Fig. 7. (A) Carbonate ion substitution relative to distance from a pore decayed exponentially (B, C) MMP-13 expression and collagen cross-linking showed similar co-localization patterns with highest expression occurring within 5–10 μm of pore edges.

It is important to note that our data only showed insignificant increases in osteocyte lacunar size. However, this does not exclude the possibility of osteocytic remodeling as MMP-13 expression, collagen cross-linking changes, and carbonate ion substitution were co-localized near lacunae and decayed exponentially as a function of distance from the pore. This is consistent with recent findings of Kerschnitzki et al., who reported that a gradient in mineral mass density exists at the lacunar boundary suggesting that mineral exchange occurs at this interface [57]. Carbonate substitution of only a few angstroms of phosphate per osteocyte would have significant effects on systemic ion levels [58,59] and explain why we didn't observe a net change in lacunar size.

TRAP activity was also associated with osteocytes, consistent with previous observations during lactation [49]. It should be noted that despite a dramatic increase in TRAP-positive osteoclasts in HYP mice, there is little evidence of resorption pits typical of osteoclast-mediated bone resorption. It is interesting to consider the possibility that the high phosphatase activity of TRAP itself may be involved in the hydrolysis of phosphate from alternative endogenous noncollagenous phosphoproteins such as osteopontin and bone sialoprotein [60].

The observed increase in MMP-13 in this study's pregnant WT mice could be in preparation for lactation as these samples were representative of the end of pregnancy. Together with cortical TRAP activity, the

data suggest WT mice also use this mechanism of perilacunar mineral turnover to provide mineral without osteoclast resorption in cortical bone (i.e., net cortical bone loss) in addition to classic osteoclast remodeling in trabecular bone. HYP mice continue this unique perilacunar mineral turnover throughout lactation as osteoclast resorption alone is not enough to meet mineral demand due to lack of trabecular bone mineral surfaces. At the end of lactation, WT had decreased TRAP activity, as mineral demand has been met and recovery has begun.

4.3. Limitations

The use of a mouse model may be limited because of the predominant lamellar cortical structure and the lack of Haversian remodeling in mice. Thus, it is unknown whether data from this study can be extrapolated to Haversian bone. Also, use of micro-CT to detect changes in cortical porosity in HYP mice may create errors in thresholding due to the severe osteomalacia. However, histology and histomorphometry verified these results. Additionally, tracking of phosphate from bone into circulation, placenta and breast milk could not be done. Thus, we could not confirm if cortical bone was indeed the source of the phosphate supplied to the fetuses and pups. Lastly, increasing the sample sizes and raising statistical power may enable the identification of

additional group differences specifically the trends seen in lacunar volume during lactation.

4.4. Summary

Taken together, these data suggest that increased intracortical mineral remodeling also contributes to maintaining phosphate levels during periods of high mineral demand. Our data suggest a higher mobilization of bone-derived phosphate and increased incorporation of carbonate into the calcium phosphate crystal complex during periods of high phosphate demand. We postulate that in conjunction with increased osteocyte expression of MMP-13, mineralized surfaces within cortical bone serve as a resource of mineral that can be resorbed to meet maternal mineral demands. Understanding the mechanisms of skeletal contribution to mineral homeostasis is important to improving the treatment and prevention of fracture risk and bone fragility for female patients with XLH, but also provides important insight into the role and unique adaptations of the maternal skeleton to the demands of fetal development and the needs of postnatal nutrition.

Acknowledgments

This work was supported in part by the EU Marie Curie International Outgoing Fellowship PIOF-GA-2012-328731 (to H.E.K.). The authors gratefully thank Thomas O. Carpenter, MD, for scientific discussions and suggestions. We thank Bruce Ellis, Caren Gundberg, Ph.D., and Christine Simpson for their technical assistance and we thank the Yale Orthopaedics Histology Lab for histological preparation. We also thank Karl Jepsen, Ph.D., and the University of Michigan Orthopaedic Research Laboratories for use of the high-resolution micro-CT. Use of the National Synchrotron Light Source, Brookhaven National Laboratory, was supported by the U.S. Department of Energy, Office of Science, Office of Basic Energy Sciences, under Contract No. DE-AC02-98CH10886.

References

- [1] C.S. Kovacs, Calcium and bone metabolism disorders during pregnancy and lactation, *Endocrinol. Metab. Clin. N. Am.* 40 (2011) 795–826.
- [2] C.S. Kovacs, H.M. Kronenberg, Maternal-fetal calcium and bone metabolism during pregnancy, puerperium, and lactation, *Endocr. Rev.* 18 (1997) 832–872.
- [3] C.S. Kovacs, Vitamin D in pregnancy and lactation: maternal, fetal, and neonatal outcomes from human and animal studies, *Am. J. Clin. Nutr.* 88 (2008) 520S–528S.
- [4] M.S. Ardawi, H.A. Nasrat, H.S. BA'Aqueel, Calcium-regulating hormones and parathyroid hormone-related peptide in normal human pregnancy and postpartum: a longitudinal study, *Eur. J. Endocrinol.* 137 (1997) 402–409.
- [5] N.A. Cross, L.S. Hillman, S.H. Allen, G.F. Krause, N.E. Vieira, Calcium homeostasis and bone metabolism during pregnancy, lactation, and postweaning: a longitudinal study, *Am. J. Clin. Nutr.* 61 (1995) 514–523.
- [6] T. Dahlman, H.E. Sjöberg, E. Bucht, Calcium homeostasis in normal pregnancy and puerperium. A longitudinal study, *Acta Obstet. Gynecol. Scand.* 73 (1994) 393–398.
- [7] S.J. Gallacher, W.D. Fraser, O.J. Owens, F.J. Dryburgh, F.C. Logue, A. Jenkins, J. Kennedy, I.T. Boyle, Changes in calciotropic hormones and biochemical markers of bone turnover in normal human pregnancy, *Eur. J. Endocrinol.* 131 (1994) 369–374.
- [8] N. Rasmussen, A. Frolich, P.J. Hornnes, L. Hegedus, Serum ionized calcium and intact parathyroid hormone levels during pregnancy and postpartum, *Br. J. Obstet. Gynaecol.* 97 (1990) 857–859.
- [9] M. Turner, P.E. Barre, A. Benjamin, D. Goltzman, M. Gascon-Barre, Does the maternal kidney contribute to the increased circulating 1,25-dihydroxyvitamin D concentrations during pregnancy? *Miner. Electrolyte Metab.* 14 (1988) 246–252.
- [10] H.J. Singh, N.H. Mohammad, A. Nila, Serum calcium and parathormone during normal pregnancy in Malay women, *J. Matern. Fetal Med.* 8 (1999) 95–100.
- [11] J. Cornish, K.E. Callon, G.C. Nicholson, I.R. Reid, Parathyroid hormone-related protein-(107–139) inhibits bone resorption in vivo, *Endocrinology* 138 (1997) 1299–1304.
- [12] M. Sowers, Pregnancy and lactation as risk factors for subsequent bone loss and osteoporosis, *J. Bone Miner. Res.* 11 (1996) 1052–1060.
- [13] Carpenter TO, New perspectives on the biology and treatment of X-linked hypophosphatemic rickets, *Pediatr. Clin. N. Am.* 44 (1997) 443–466.
- [14] G. Liang, J. Vanhouten, C.M. Macica, An atypical degenerative osteoarthropathy in Hyp mice is characterized by a loss in the mineralized zone of articular cartilage, *Calcif. Tissue Int.* 89 (2011) 151–162.
- [15] T. Nesbitt, I. Fujiwara, R. Thomas, Z.S. Xiao, L.D. Quarles, M.K. Drezner, Coordinated maturational regulation of PHEX and renal phosphate transport inhibitory activity: evidence for the pathophysiological role of PHEX in X-linked hypophosphatemia, *J. Bone Miner. Res.* 14 (1999) 2027–2035.
- [16] Z.S. Xiao, M. Crenshaw, R. Guo, T. Nesbitt, M.K. Drezner, L.D. Quarles, Intrinsic mineralization defect in Hyp mouse osteoblasts, *Am. J. Physiol.* 275 (1998) E700–E708.
- [17] TheHYPConsortium, A gene (PEX) with homologies to endopeptidases is mutated in patients with X-linked hypophosphatemic rickets. The HYP Consortium, *Nat. Genet.* 11 (1995) 130–136.
- [18] S. Liu, J. Zhou, W. Tang, X. Jiang, D.W. Rowe, L.D. Quarles, Pathogenic role of Fgf23 in Hyp mice, *Am. J. Physiol. Endocrinol. Metab.* 291 (2006) E38–E49.
- [19] T. Hayashibara, T. Hiraga, A. Sugita, L. Wang, K. Hata, T. Ooshima, T. Yoneda, Regulation of osteoclast differentiation and function by phosphate: potential role of osteoclasts in the skeletal abnormalities in hypophosphatemic conditions, *J. Bone Miner. Res.* 22 (2007) 1743–1751.
- [20] T. Ono, H. Tanaka, T. Yamate, Y. Nagai, T. Nakamura, Y. Seino, 24R,25-dihydroxyvitamin D3 promotes bone formation without causing excessive resorption in hypophosphatemic mice, *Endocrinology* 137 (1996) 2633–2637.
- [21] J.J. Wysolmerski, Osteocytic osteolysis: time for a second look? *Bonekey Rep* 1 (2012) 229.
- [22] N. Otsu, A threshold selection method from gray-level histograms, *IEEE 62-6* (1979).
- [23] S.M. Tommasini, A. Trinward, A.S. Acerbo, F. De Carlo, L.M. Miller, S. Judex, Changes in intracortical microporosities induced by pharmaceutical treatment of osteoporosis as detected by high resolution micro-CT, *Bone* 50 (2012) 596–604.
- [24] R.G. Bannister, F.C. Romanul, The localization of alkaline phosphatase activity in cerebral blood vessels, *J. Neurol. Neurosurg. Psychiatry* 26 (1963) 333–340.
- [25] S.Y. Tang, R.P. Herber, S.P. Ho, T. Alliston, Matrix metalloproteinase-13 is required for osteocytic perilacunar remodeling and maintains bone fracture resistance, *J. Bone Miner. Res.* 27 (2012) 1936–1950.
- [26] C.A. Brownstein, J. Zhang, A. Stillman, B. Ellis, N. Troiano, D.J. Adams, C.M. Gundberg, R.P. Lifton, Carpenter TO, Increased bone volume and correction of HYP mouse hypophosphatemia in the Klotho/HYP mouse, *Endocrinology* 151 (2010) 492–501.
- [27] N.P. Camacho, L. Hou, T.R. Toledano, W.A. Ilg, C.F. Brayton, C.L. Raggio, L. Root, A.L. Boskey, The material basis for reduced mechanical properties in oim mice bones, *J. Bone Miner. Res.* 14 (1999) 264–272.
- [28] S.J. Gadeleta, A.L. Boskey, E. Paschalis, C. Carlson, F. Menschik, T. Baldini, M. Peterson, C.M. Rimmac, A physical, chemical, and mechanical study of lumbar vertebrae from normal, ovariectomized, and nandrolone decanoate-treated cynomolgus monkeys (*Macaca fascicularis*), *Bone* 27 (2000) 541–550.
- [29] W.F. Neuman, M.W. Neuman, The Chemical Dynamics of Bone Mineral, The University of Chicago Press, Chicago, 1958.
- [30] A. Awonusi, M.D. Morris, M.M. Tecklenburg, Carbonate assignment and calibration in the Raman spectrum of apatite, *Calcif. Tissue Int.* 81 (2007) 46–52.
- [31] R.M. Biltz, E.D. Pellegrino, The nature of bone carbonate, *Clin. Orthop. Relat. Res.* 279–92 (1977).
- [32] E.D. Pellegrino, R.M. Biltz, J.M. Letteri, Inter-relationships of carbonate, phosphate, monohydrogen phosphate, calcium, magnesium and sodium in uraemic bone: comparison of dialysed and non-dialysed patients, *Clin. Sci. Mol. Med.* 53 (1977) 307–316.
- [33] Y. Ma, M. Samaraweera, S. Cooke-Hubley, B.J. Kirby, A.C. Karaplis, B. Lanske, C.S. Kovacs, Neither absence nor excess of FGF23 disturbs murine fetal-placental phosphorus homeostasis or prenatal skeletal development and mineralization, *Endocrinology* 155 (2014) 1596–1605.
- [34] Y. Ohata, M. Yamazaki, M. Kawai, N. Tsugawa, K. Tachikawa, T. Koinuma, K. Miyagawa, A. Kimoto, M. Nakayama, N. Namba, H. Yamamoto, T. Okano, K. Ozono, T. Michigami, Elevated fibroblast growth factor 23 exerts its effects on placenta and regulates vitamin D metabolism in pregnancy of Hyp mice, *J. Bone Miner. Res.* 29 (2014) 1627–1638.
- [35] B.J. Kirby, Y. Ma, H.M. Martin, K.L. Buckle Favaro, A.C. Karaplis, C.S. Kovacs, Upregulation of calcitriol during pregnancy and skeletal recovery after lactation do not require parathyroid hormone, *J. Bone Miner. Res.* 28 (2013) 1987–2000.
- [36] L. Ardeshipour, S. Brian, P. Dann, J. VanHouten, J. Wysolmerski, Increased PTHrP and decreased estrogens alter bone turnover but do not reproduce the full effects of lactation on the skeleton, *Endocrinology* 151 (2010) 5591–5601.
- [37] M.J. Horwitz, M.B. Tedesco, S.M. Sereika, M.A. Syed, A. Garcia-Ocana, A. Bisello, B.W. Hollis, C.J. Rosen, J.J. Wysolmerski, P. Dann, C. Gundberg, A.F. Stewart, Continuous PTH and PTHrP infusion causes suppression of bone formation and discordant effects on 1,25(OH)₂ vitamin D, *J. Bone Miner. Res.* 20 (2005) 1792–1803.
- [38] D.V. Ajibade, P. Dhawan, A.J. Fechner, M.B. Meyer, J.W. Pike, S. Christakos, Evidence for a role of prolactin in calcium homeostasis: regulation of intestinal transient receptor potential vanilloid type 6, intestinal calcium absorption, and the 25-hydroxyvitamin D(3) 1 α hydroxylase gene by prolactin, *Endocrinology* 151 (2010) 2974–2984.
- [39] C.J. Robinson, E. Spanos, M.F. James, J.W. Pike, M.R. Haussler, A.M. Makeen, C.J. Hillyard, I. MacIntyre, Role of prolactin in vitamin D metabolism and calcium absorption during lactation in the rat, *J. Endocrinol.* 94 (1982) 443–453.
- [40] E. Spanos, K.W. Colston, I.M. Evans, L.S. Galante, S.J. Macauley, I. MacIntyre, Effect of prolactin on vitamin D metabolism, *Mol. Cell. Endocrinol.* 5 (1976) 163–167.
- [41] M.J. Econs, B. Lobaugh, M.K. Drezner, Normal calcitonin stimulation of serum calcitriol in patients with X-linked hypophosphatemic rickets, *J. Clin. Endocrinol. Metab.* 75 (1992) 408–411.
- [42] E.S. Liu, Carpenter TO, C.M. Gundberg, C.A. Simpson, K.L. Insogna, Calcitonin administration in X-linked hypophosphatemia, *N. Engl. J. Med.* 364 (2011) 1678–1680.
- [43] T. Shinki, Y. Ueno, H.F. DeLuca, T. Suda, Calcitonin is a major regulator for the expression of renal 25-hydroxyvitamin D3-1 α hydroxylase gene in normocalcemic rats, *Proc. Natl. Acad. Sci. U. S. A.* 96 (1999) 8253–8258.
- [44] J.P. Woodrow, C.J. Sharpe, N.J. Fudge, A.O. Hoff, R.F. Gagel, C.S. Kovacs, Calcitonin plays a critical role in regulating skeletal mineral metabolism during lactation, *Endocrinology* 147 (2006) 4010–4021.
- [45] F. Barrere, C.A. van Blitterswijk, K. de Groot, Bone regeneration: molecular and cellular interactions with calcium phosphate ceramics, *Int. J. Nanomedicine* 1 (2006) 317–332.

- [46] C.S. Kovacs, Osteoporosis presenting in pregnancy, puerperium, and lactation, *Curr. Opin. Endocrinol. Diabetes Obes.* 21 (2014) 468–475.
- [47] C.C. Hayslip, T.A. Klein, H.L. Wray, W.E. Duncan, The effects of lactation on bone mineral content in healthy postpartum women, *Obstet. Gynecol.* 73 (1989) 588–592.
- [48] G.N. Kent, R.I. Price, D.H. Gutteridge, M. Smith, J.R. Allen, C.I. Bhagat, M.P. Barnes, C.J. Hickling, R.W. Retallack, S.G. Wilson, et al., Human lactation: forearm trabecular bone loss, increased bone turnover, and renal conservation of calcium and inorganic phosphate with recovery of bone mass following weaning, *J. Bone Miner. Res.* 5 (1990) 361–369.
- [49] H. Qing, L. Ardeshirpour, P.D. Pajevic, V. Dusevich, K. Jahn, S. Kato, J. Wysolmerski, L.F. Bonewald, Demonstration of osteocytic perilacunar/canalicular remodeling in mice during lactation, *J. Bone Miner. Res.* 27 (2012) 1018–1029.
- [50] S. Kaya, J. Basta-Pljakic, Z. Seref-Ferlengez, W.Y. Cheung, R. Majeska, S. Fritton, S. Yakar, M.B. Schaffler, Local bone tissue mechanical properties change without remodeling: A study of lactating mice, *J. Bone Miner. Res.* 29 (2014).
- [51] P.H. Wright, J.O. Jowsey, R.A. Robb, Osteocyte lacunar area in normal bone, hyperparathyroidism, renal disease, and osteoporosis, *Surg. Forum* 29 (1978) 558–559.
- [52] P. Bianco, E. Bonucci, Endosteal surfaces in hyperparathyroidism: an enzyme cytochemical study on low-temperature-processed, glycol-methacrylate-embedded bone biopsies, *Virchows Arch. A Pathol. Anat. Histopathol.* 419 (1991) 425–431.
- [53] A. Yajima, M. Inaba, Y. Tominaga, Y. Nishizawa, K. Ikeda, A. Ito, Increased osteocyte death and mineralization inside bone after parathyroidectomy in patients with secondary hyperparathyroidism, *J. Bone Miner. Res.* 25 (2010) 2374–2381.
- [54] M. Inada, Y. Wang, M.H. Byrne, M.U. Rahman, C. Miyaura, C. Lopez-Otin, S.M. Krane, Critical roles for collagenase-3 (Mmp13) in development of growth plate cartilage and in endochondral ossification, *Proc. Natl. Acad. Sci. U.S.A.* 101 (2004) 17192–17197.
- [55] D. Stickens, D.J. Behonick, N. Ortega, B. Heyer, B. Hartenstein, Y. Yu, A.J. Fosang, M. Schorpp-Kistner, P. Angel, Z. Werb, Altered endochondral bone development in matrix metalloproteinase 13-deficient mice, *Development* 131 (2004) 5883–5895.
- [56] E.P. Paschalis, R. Recker, E. DiCarlo, S.B. Doty, E. Atti, A.L. Boskey, Distribution of collagen cross-links in normal human trabecular bone, *J. Bone Miner. Res.* 18 (2003) 1942–1946.
- [57] M. Kerschnitzki, P. Kollmannsberger, M. Burghammer, G.N. Duda, R. Weinkamer, W. Wagermaier, P. Fratzl, Architecture of the osteocyte network correlates with bone material quality, *J. Bone Miner. Res.* 28 (2013) 1837–1845.
- [58] G. Marotti, M. Ferretti, F. Remaggi, C. Palumbo, Quantitative evaluation on osteocyte canalicular density in human secondary osteons, *Bone* 16 (1995) 125–128.
- [59] H. Qing, L.F. Bonewald, Osteocyte remodeling of the perilacunar and pericanalicular matrix, *Int. J. Oral Sci.* 1 (2009) 59–65.
- [60] H. Bull, P.G. Murray, D. Thomas, A.M. Fraser, P.N. Nelson, Acid phosphatases, *Mol. Pathol.* 55 (2002) 65–72.